서울도시연구 제8권 제3호 2007. 9, 논문 -Original Paper- pp. 71～83. 71

Spatiotemporal Hotspot Detection Using G Statistics

- A Case of Traffic Accidents in East Japan -

Yang-Won Lee*

G통계량을 이용한 시공간 핫스팟 탐지기법

- 일본 관동지방의 교통사고 사례연구 -

이 양 원*

ABSTRACT : This paper describes a statistical method of applying local spatial autocorrelation measures to the spatiotemporal hotspot detection in geographic phenomena. By modifying local G statistics into a spatiotemporal version, a hotspot detection technique can be extended to the space-time dimension. The weighting schemes required for the spatiotemporal G statistics are built by combining the concepts of distance decay and time decay, and each region's possibility of spatiotemporal hotspot is derived from the G statistics with the spatiotemporal weighting schemes. A primary hotspot and secondary hotspots are delineated using a contiguity-dominance model, and the spatiotemporal hotspots are represented in the three dimension composed of XY-plane(space) and T-axis(time). The feasibility of the proposed method was tested by the analyses on the time-series data of traffic accidents in East Japan, 2000-2005. In the experiment, moderate autocorrelation tendencies were observed at statistically significant levels, and a primary hotspot and three secondary hotspots were found in Tokyo-to, Gunma-ken, and Kanagawa-ken. The spatiotemporal hotspots simultaneously demonstrate spatial and temporal extents of a prevailing geographic phenomenon and provide consecutive cluster information composed of “when” and “where”.

Key Words : spatiotemporal autocorrelation, spatiotemporal hotspots, geographic information systems

요약 : 이 논문에서는 공간자기상관의 통계적 특성을 응용하여 지리현상에서의 시공간 핫스팟을 탐지하는 기법을 제시한다. 국지적 공간자기상관의 지표인 G통계량은 시공간 가중치와 결합하여 시공간 핫스팟 탐지에 활용될 수 있다. 시공간 가중치 체계는 거리조락 및 시간조락의 개념을 반영하여 구성하고, 이를 시공간 버전의 G통계량에 도입함으로써, 각 시점, 각 단위지역의 시공간 자기상관계수를 계산한다. 인접-우세모형에 기초한 핫스팟 탐지 알고리즘은 시점 및 지역별 자기상관계수를 기준으로 시공간 핫스팟을 구획화하여 XY-T(공간-시간)의 입체로 표현한다. 2000년-2005년 일본 관동지방의 교통사고발생 시계열자료에 대한 분석을 통해 이 방법론을 테스트한 결과, 통계적으로 유의미한 수준에서 일정 정도의 자기상관 경향이 발견되었으며, 도쿄도, 군마현, 카나가와현에서 시공간 핫스팟이 탐지되었다. 시공간 핫스팟은 지리현상 발생의 공간적 및 시간적 우세범위를 동시에 표현함으로써 ‘언제 어디에서’의 연속적 클러스터 정보를 제공한다.

주제어 : 시공간 자기상관, 시공간 핫스팟, 지리정보시스템

* Postdoctoral Researcher, Center for Spatial Information Science, University of Tokyo(도쿄대 공간정보과학연구센터 연구원), jwlee@iis.u-tokyo.ac.jp.

Ⅰ. Introduction

The attributes of geographic phenomena tend to vary over space and time. From these varying patterns, we often find spatially gathered areas where the density of a phenomenon is significantly high or considerably low. The high parts and the low parts can show a clustered pattern, which indicates a spatially autocorrelated distribution. Spatial autocorrelation arises when the value of a variable at a location is related to the values of the same variable at nearby locations(Wulder and Boots, 1998). Thus, the measurements of spatial autocorrelation consider both locational and attribute information(Goodchild, 1986). The spatial autocorrelation has been modeled in the global indices by Moran(1948), Geary(1954), and Getis and Ord(1992), and the local indices by Anselin(1995; 1996) and Ord and Getis(1995). Global measures of spatial autocorrelation produce a single value that indicates the presence of spatial autocorrelation in the whole area. However, since the global value may not be universally applicable throughout the whole area, the local measures alternatively examine spatial dependence in subsets, focusing on the variations within the study area(Fotheringham, 1997; Fotheringham and Brunsdon, 1999; Boots, 2003).

Therefore, the local measures of spatial autocorrelation can be used to reveal where high clusters(hotspots) and low clusters(cold spots) are located in the uneven distribution of a phenomenon(Getis and Ord, 1996). Especially hotspot, a set of distinctively concentrated areas, is of interest to the studies on discovering a spatial structure of rare and risky phenomena such as crime, disease, and pollution(Messner and Anselin, 2004). However, so far, little attention has been given to the use of local spatial autocorrelation for the hotspot detection in a spatiotemporal dimension. Although both spatiality and temporality are the key to understanding geographical process(Yao, 2003), there have been difficulties in formulating the spatiotemporal relationships among geographic phenomena and in utilizing the indices of local spatial autocorrelation in a spatiotemporal way. When compared to a spatial hotspot that shows highly concentrated areas for one time point, the spatiotemporal hotspot can demonstrate the extents to which a phenomenon prevails spatially and temporally as well.

This paper describes a statistical method of applying spatial autocorrelation to the spatiotemporal hotspot detection in geographic phenomena. Local G statistics by Ord and Getis were modified into a space-time version, and a contiguity-dominance model was employed for the discovery of highly concentrated areas, using the spatiotemporal autocorrelation measures of each administrative region. The weighting schemes for spatiotemporal proximity were built by combining the concepts of distance decay and time decay. Distance is parameterized in the G statistics, so that the statistics are suited to distance effects of spatial autocorrelation. The G statistics can be also used in integrating time effects into distance effects to examine the characteristics of spatiotemporal autocorrelation because time can be another weight in G statistics. Using the G statistics with the modified weighting schemes, spatiotemporal

hotspots are sought based on a contiguity-dominance model, which recursively searches for contiguous and dominant spatiotemporal neighbors, starting from a core node(the node with highest value). A spatiotemporal hotspot continues to incorporate neighboring high-value nodes until the components of the hotspot possess an adequate internal homogeneity and have a sufficient heterogeneity with external nodes.

The applicability of the proposed method was tested by the analyses on time-series data of the traffic accidents in East Japan(Figure 1), 2000-2005. In general, the occurrence of a single traffic accident is regarded as random in space and time. However, the non-uniform distributions of traffic volume and population density(Okabe et al., 2006) may cause regional differences in the occurrence rate of traffic accidents and bring about the formation of hotspots. A number of research has dealt with the spatial clustering of traffic accidents, in terms of road networks or administrative regions(e.g., McGuigan, 1981; Maher and Mountain, 1988; Nicholson, 1989; Levine et al., 1995; Hong, 1998; Flahaut et al., 2003; Steenberghen et al., 2004; Yamada and Thill, 2004; Sabel et al., 2005; Aerts et al., 2006). In this paper, the traffic accident data was used as an example of the feasibility test for the proposed method. If a visual proof of high-value cluster is found and a tendency of spatial autocorrelation is observed at a statistically significant level, the spatiotemporal hotspot detection using local G statistics can be applied to the time-series traffic accidents. Although the strength of global autocorrelation in data is not so strong, the local measures can account for spatially and temporally concentrated extents that cannot be explained by global measures.

Figure 1. Map of Administrative Regions in East Japan

Ⅱ. Methods

The statistical method for spatiotemporal hotspot detection consists of (i) weighting scheme of spatiotemporal proximity based on distance decay and time decay, (ii) spatiotemporally weighted G statistics that provide each region's possibility of high cluster, and (iii) contiguity-dominance model to discover spatiotemporal hotspots.

1. Spatiotemporal Proximity

The proximity among geographic entities is typically defined based on the spatial relationships such as distance, geometry, and topology(Bailey and Gatrell, 1995; Lee and Wong, 2001; Bera and Claramunt, 2003; Park, 2004). Temporal proximity can be combined with the spatial proximity on a distance-time basis. Suppose a geographic feature

at the space s and the time t is denoted as L_s^t. The spatiotemporal proximity between L_s^t and L_{s+1}^{t+1} (one spatial lag and one temporal lag) can be determined by the spatial proximity between L_s^t and L_{s+1}^t (one spatial lag at the same time point) and the temporal proximity between L_{s+1}^t and L_{s+1}^{t+1} (one temporal lag at the same location), as follows.

$$stProx(L_s^t, L_{s+1}^{t+1}) = sProx(L_s^t, L_{s+1}^t) \cdot tProx(L_{s+1}^t, L_{s+1}^{t+1})$$

It can be also expressed using the temporal relationship with a temporal neighbor at the same location, and the spatial relationship with a spatial neighbor at the same time point, as follows.

$$stProx(L_s^t, L_{s+1}^{t+1}) = tProx(L_s^t, L_s^{t+1}) \cdot sProx(L_s^{t+1}, L_{s+1}^{t+1})$$

Thus, the weight of spatiotemporal proximity can be represented in a general form using a spatial proximity function $f(s)$ and a temporal proximity function $g(t)$: $w = f(s) \cdot g(t) = g(t) \cdot f(s)$ and $\iint f(s) \cdot g(t) ds dt = 1$. Figure 2 shows the concept of the spatiotemporal proximity, and the $f(s)$ and $g(t)$ can be modeled in the linear or exponential method(Figure 3). Natural numbers such as 2 and 3 can be used as the exponent(Upton, 1990).

2. Spatiotemporally-weighted G Statistics

G statistics are the distance-based indices of spatial autocorrelation. $G_i(d)$ and $G_i^*(d)$ indicate

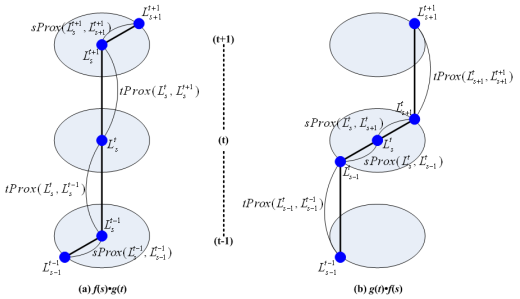

Figure 2. Combining Spatial and Temporal Proximities

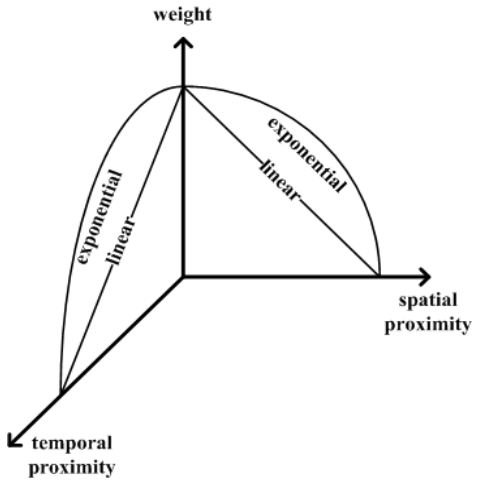

Figure 3. Weighting Methods for Spatial and Temporal Proximity

the degree to which a location i is surrounded by a cluster of high or low values, for a chosen critical distance d. The $G_i(d)$ excludes the value at i(self-neighbor) from the summation while the $G_i^*(d)$ includes the value at i. Positive $G_i(d)$ and $G_i^*(d)$ indicate the spatial clustering of high values whereas negative $G_i(d)$ and $G_i^*(d)$ mean the spatial clustering of low values. The G statistics are originally a spatial measure, and they can be used as a spatiotemporal indicator of autocorrelation, by importing the weighting scheme of spatiotemporal proximity, as follows.

$$G_i(d,t) = \frac{\sum_{j=1,j\neq i}^{n} w_{ij}(d,t)x_j - \bar{x}\sum_{j=1,j\neq i}^{n} w_{ij}(d,t)}{S(i)\sqrt{\frac{(n-1)\sum_{j=1,j\neq i}^{n} w_{ij}^2(d,t) - \left(\sum_{j=1,j\neq i}^{n} w_{ij}(d,t)\right)^2}{n-2}}}$$

where x_j is the j-th spatiotemporal neighbor for i; n is the number of spatiotemporal neighbors for i;

$$\bar{x} = \frac{\sum_{j=1,j\neq i}^{n} x_j}{n-1}; \text{ and}$$

$$S(i) = \sqrt{\frac{\sum_{j=1,j\neq i}^{n} x_j}{n-1} - (\bar{x}_i)^2}.$$

$$G_i^*(d,t) = \frac{\sum_{j=1}^{n} w_{ij}(d,t)x_j - \bar{x}\sum_{j=1}^{n} w_{ij}(d,t)}{S\sqrt{\frac{n\sum_{j=1}^{n} w_{ij}^2(d,t) - \left(\sum_{j=1}^{n} w_{ij}(d,t)\right)^2}{n-1}}}$$

where x_j is the j-th spatiotemporal neighbor for i; n is the number of spatiotemporal neighbors for i;

$$\bar{x} = \frac{\sum_{j=1}^{n} x_j}{n}; \text{ and}$$

$$S = \sqrt{\frac{\sum_{j=1}^{n} x_j}{n} - (\bar{x})^2}.$$

3. Spatiotemporal Hotspot Detection

In this paper, a spatiotemporal hotspot is defined as a set of geographic entities which are spatiotemporally neighboring and whose G values are significantly high. Here, the spatiotemporal neighbors denote the regions that are spatially adjacent and temporally consecutive. In discovering hotspots from the spatiotemporal neighbor structure, a contiguity-dominance model was used. Starting from the core node(region) with the maximum G value, the discovery algorithm investigates whether the spatiotemporal neighbors meet the criteria of dominance: for example, 2σ or 95th percentile can be used as a threshold value, on a distribution basis. Once a new eligible node is added to the hotspot, its spatiotemporal neighbors are also examined to determine if the strength of the neighbors is dominant enough. This procedure is repeated until all appropriate nodes are attached to the hotspot(Figure 4), so that the hotspot can have an inner homogeneity distinguished from outer space-time.

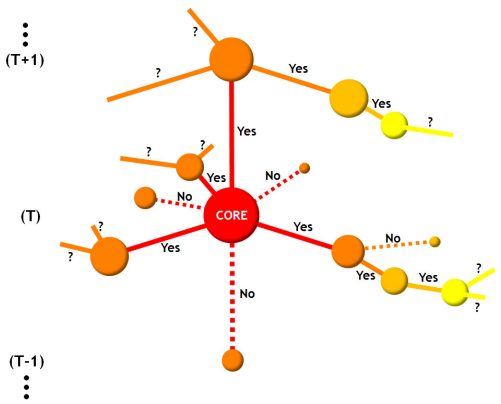

Figure 4. Spatiotemporal Hotspot Detection Using a Contiguity-Dominance Model

The hotspot created from the core node is regarded as a primary hotspot. After discovering the primary hotspot, secondary hotspots are scrutinized for the remaining area. The initial space-time point of a secondary hotspot is decided as the node with the maximum G value in the remaining area. Scanning high-value neighbors

follows the same step as in the primary hotspot. There can be several secondary hotspots. A secondary hotspot is considered eligible only if its extent is sufficiently large and the distance from the primary hotspot is far enough. In the simulation experiment, a 95th percentile and a 90th percentile were used as the criteria for the primary hotspot and the secondary hotspots, respectively.

Ⅲ. Simulation Experiment

1. Data Exploration

In general, East Japan indicates the areas including Ibaraki-ken(茨城縣), Tochigi-ken(栃木縣), Gunma-ken(群馬縣), Saitama-ken(埼玉縣), Chiba-ken(千葉縣), Tokyo-to(東京都), and Kanagawa-ken(神奈川縣). Time-series data of the number of traffic accidents in 356 administrative regions of East Japan was analyzed in this experiment. The data obtained from the web site of MLIT(Ministry of Land, Infrastructure and Transport) was aggregated on a yearly basis between 2000 and 2005. First, the histograms classified by Jenks' natural break method were drawn to capture the overall distribution of the number of traffic accidents(Figure 5).

The histograms of every year show a skewed distribution, with the existence of very high-value regions. In order to see if the high-value regions gather, choropleth maps of the number of traffic accidents per 10,000 persons were drawn. In Figure 6, bumps of high values seem clustered to some degree.

Then, for a statistical test of the spatial clustering tendency, global Moran's I and Geary's C were calculated. The range of Moran's I is between -1 and 1. The value -1 indicates an extremely negative autocorrelation while 1 means an extremely positive autocorrelation. Geary's C is inversely related to Moran's I and ranges from 0 to 2. The value 0 corresponds to extreme positive whereas 2 represents extreme negative.

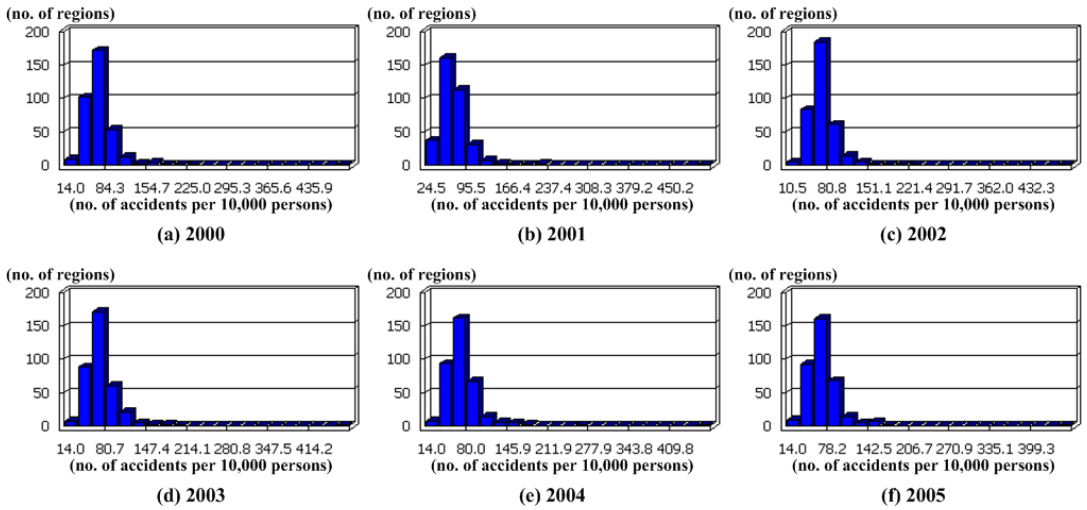

Figure 5. Histograms of the Number of Traffic Accidents per 10,000 Persons

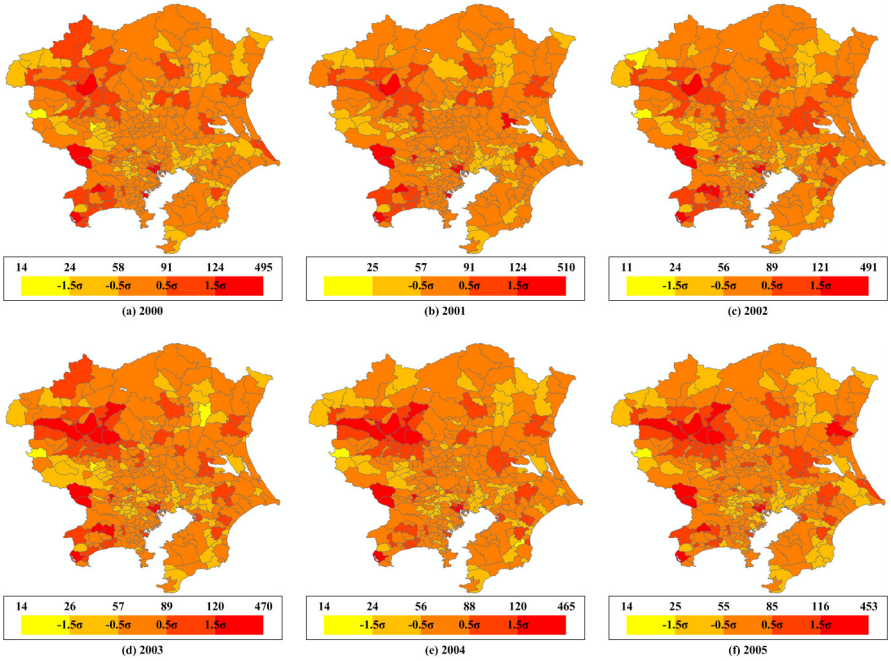

Figure 6. Choropleth Maps of the Number of Traffic Accidents per 10,000 Persons

$$I=\frac{n\sum_{i=1}^{n}\sum_{j=1,j\neq i}^{n}w_{ij}(x_i-\bar{x})(x_j-\bar{x})}{W\sum_{i=1}^{n}(x_i-\bar{x})^2}$$

$$C=\frac{(n-1)\sum_{i=1}^{n}\sum_{j=1,j\neq i}^{n}w_{ij}(x_i-x_j)^2}{2W\sum_{i=1}^{n}(x_i-\bar{x})^2}$$

where $\bar{x}=\frac{\sum_{i=1}^{n}x_i}{n}$ and $W=\sum_{i=1}^{n}\sum_{j=1}^{n}w_{ij}$.

As the weighting matrices for the global indices, a binary contiguity and a KNN(k nearest neighbor) method were used in this test. The statistics in Table 1 and Table 2 show that the traffic accidents in East Japan are somewhat spatially autocorrelated at statistically significant levels, though the overall tendencies are not so strong.

〈Table 1〉 Global Indices of Spatial Autocorrelation with a Binary Contiguity Matrix

	2000	2001	2002	2003	2004	2005
Moran's I	0.2482[a]	0.2589[a]	0.2421[a]	0.2711[a]	0.2632[a]	0.2753[a]
Geary's C	0.7046[b]	0.6879[b]	0.7131[b]	0.7007[b]	0.6925[b]	0.6939[b]

note) a: p-value = 0; b :p-value < 0.01.

〈Table 2〉 Global Indices of Spatial Autocorrelation with K Nearest Neighbor Matrices

		2000	2001	2002	2003	2004	2005
Moran's I	k=2	0.3079[a]	0.3369[a]	0.3156[a]	0.3287[a]	0.3354[a]	0.3384[a]
	k=3	0.3002[a]	0.3169[a]	0.3025[a]	0.3300[a]	0.3223[a]	0.3270[a]
	k=4	0.2703[a]	0.2838[a]	0.2655[a]	0.2941[a]	0.2874[a]	0.2947[a]
	k=5	0.2665[a]	0.2760[a]	0.2597[a]	0.2835[a]	0.2728[a]	0.2860[a]
Geary's C	k=2	0.7858[c]	0.7585[c]	0.7918[c]	0.7684[c]	0.7354[c]	0.7526[c]
	k=3	0.6860[b]	0.6635[b]	0.6941[b]	0.6678[b]	0.6438[b]	0.6582[b]
	k=4	0.7628[b]	0.7462[b]	0.7814[b]	0.7541[b]	0.7292[b]	0.7478[b]
	k=5	0.7945[b]	0.7852[b]	0.8180[b]	0.7929[b]	0.7720[b]	0.7903[b]

note) a: p-value = 0; b: p-value < 0.01; c: p-value < 0.05.

2. Spatiotemporal Hotspot Mapping

In this experiment, the spatiotemporal G statistics were first calculated using a linear weighting scheme for the spatiotemporal proximities of each region and of each year. The distances among regions were measured using polygon centroid, the mass center of a polygon, derived as follows.

$$X = \frac{\sum_{i=1}^{n}(x_i + x_{i+1})(x_i y_{i+1} - x_{i+1} y_i)}{6A}$$

$$Y = \frac{\sum_{i=1}^{n}(y_i + y_{i+1})(x_i y_{i+1} - x_{i+1} y_i)}{6A}$$

where n is the number of points that consist of a polygon; x_i and y_i are the x- and y-coordinate of i-th point; $x_{n+1} = x_1$; $y_{n+1} = y_1$; and A is the area of the polygon.

The spatiotemporally-weighted $G_i(d)$ and $G_i^*(d)$ of the traffic accidents in East Japan, 2000-2005 are presented as the choropleth maps in Figure 7 and Figure 8. Through these maps, we can see the high cluster of Gunma-ken has been growing while that of Kanagawa-ken has been diminishing, which cannot be discovered in the ratio-based usual choropleth maps for each year. Both $G_i(d)$ and $G_i^*(d)$ were produced using the spatiotemporal weighing scheme composed of the distance parameter of 20 kilometers and the time

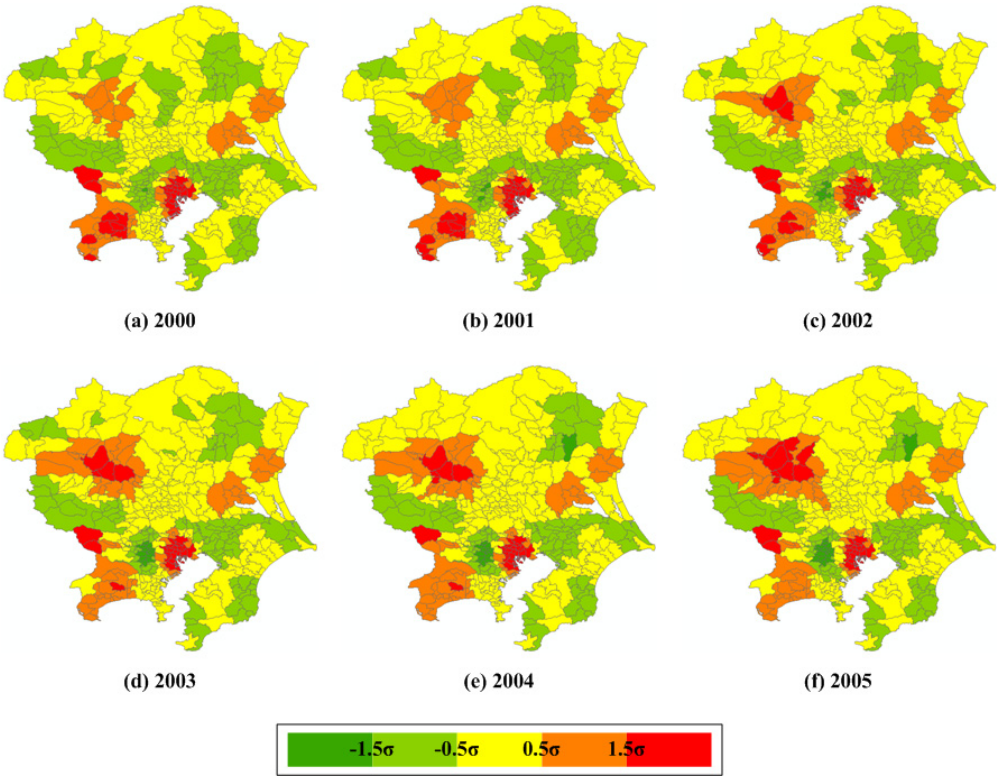

Figure 7. Spatiotemporally-weighted $G_i(d,t)$ (d < 20 km and t < ±3 yr)

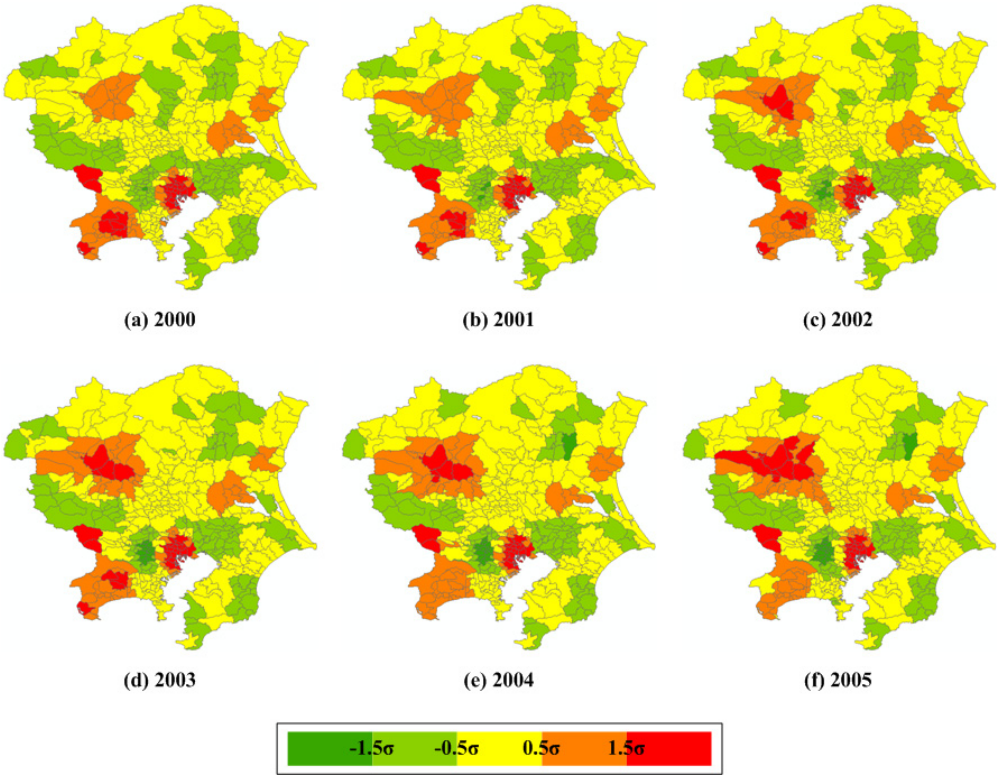

Figure 8. Spatiotemporally-weighted $G_i^*(d,t)$ (d < 20 km and t < ±3 yr)

parameter of ±3 years. These parameters are an example derived from the fact that every region has neighbor(s) within a 20-km radius, and at least half of the whole temporal range can be reached by ±3 years from any time point.

From the values of spatiotemporally weighted $G_i(d,t)$ and $G_i^*(d,t)$ for the 6 years, a primary hotspot and three secondary hotspots were found and represented in the three dimension composed of XY-plane(space) and T-axis(time). As illustrated in Figure 9(a) and Figure 10(a), the geographic location of each subregion is arranged in the XY-plane, and the years between 2000 and 2005 are displayed in the T-axis. The size of a sphere corresponds to the value of G statistics, and the spatiotemporal neighbors are connected by horizontal and vertical lines in the XY-T dimension. For convenience, the hotspots were projected to a 2D(two-dimensional) plane in Figure 9(b) and Figure 10(b). The intensity of each node in the spatiotemporal hotspots was visualized with the choroplethic color scheme based on a quartile classification(Figure 9(c) and Figure 10(c)). This intensity diagram explains "when," "where," and "how" of the components of a spatiotemporal hotspot.

In order to examine the sensitivity of the spatiotemporal weighting scheme, the exponential method for distance and time was tested with regard to $G_i(d,t)$ and $G_i^*(d,t)$. Figure 11 demonstrates the primary and secondary hotspots

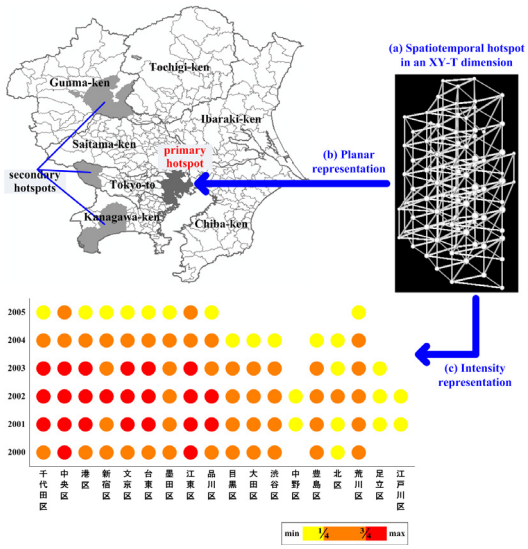

Figure 9. Spatiotemporal Hotspots Calculated Using $G_i(d,t)$

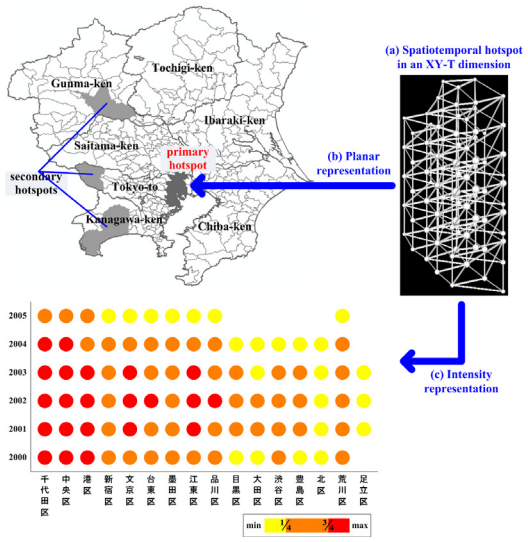

Figure 10. Spatiotemporal Hotspots Calculated Using $G_i^*(d,t)$

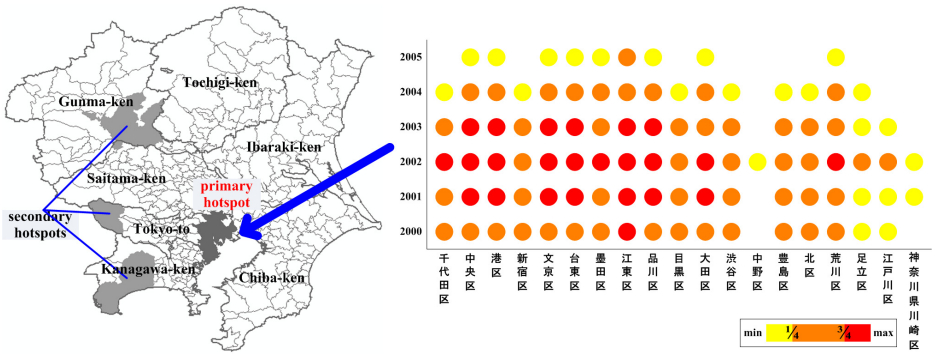

(a) Using $G_i(d,t)$

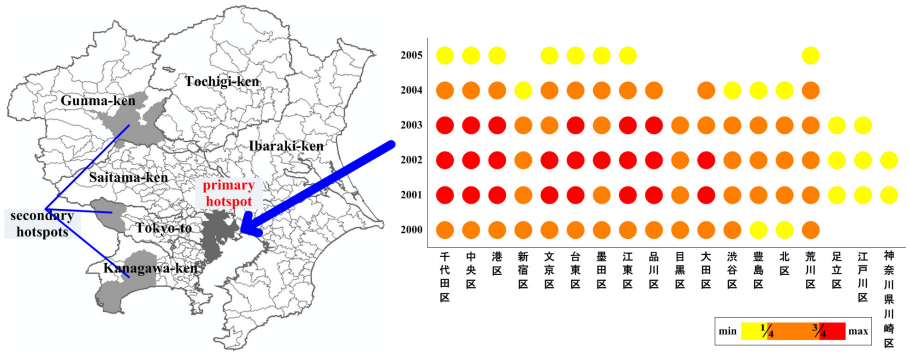

(b) Using $G_i^*(d,t)$

Figure 11. Spatiotemporal Hotspots with an Exponential Weighting Scheme(exponent = 2)

derived from the exponential weighting scheme. The hotspots by the exponential method tend to have somewhat larger spatiotemporal extents than those of the linear method. This is because an exponential curve produces a more lenient definition of neighbor, so that relatively far spatiotemporal neighbors can be also included. In addition, the hotspots by $G_i^*(d,t)$ were the subsets of the hotspots by $G_i(d,t)$, which indicates the $G_i^*(d,t)$ creates a more compact cluster because it includes self-neighbor and gives other neighbors less weights than the $G_i(d,t)$ does.

Ⅳ. Concluding Remarks

This paper discussed the application of local spatial autocorrelation measures to spatiotemporal hotspot detection. By modifying local G statistics into a spatiotemporal version, a hotspot detection technique was extended to the space-time dimension. The weighting schemes required for the spatiotemporal G statistics were built by combining the concepts of distance decay and time decay, and each region's possibility of spatiotemporal hotspot was derived from the G statistics with the spatiotemporal weighting schemes. A primary hotspot and secondary hotspots were delineated using a contiguity-dominance model, and the spatiotemporal hotspots were represented in the three dimension composed of XY-plane(space) and T-axis(time).

The feasibility of the proposed method was tested by the analyses on the time-series data of traffic accidents in East Japan, 2000-2005. Although the occurrence of a single traffic accident is considered random in space and time, the accidents aggregated by administrative region can show a clustered pattern because of the non-uniform distributions of traffic volume and population density. In the accidents data, moderate autocorrelation tendencies were observed at statistically significant levels, and the spatiotemporal hotspot detection using $G_i(d,t)$ and $G_i^*(d,t)$ was conducted with the weighting schemes by the linear and exponential methods. According to the experiment results, the $G_i^*(d,t)$ statistic and the linear weighting scheme tend to produce more compact spatiotemporal hotspots. Therefore, adaptive choices of the type of statistic, weighting scheme, and threshold value will be crucial to the use of the proposed method. Since it is not the issue of performance but the issue of selection(Park, 2004), the parameters should be adjusted depending on the purpose of study.

While spatial hotspots show the high clusters for a specific time point, the spatiotemporal hotspots simultaneously demonstrate spatial and temporal extents of a prevailing geographic phenomenon. Moreover, the spatiotemporal hotspots provide consecutive cluster information using a three-dimensional composite of "when" and "where," which cannot be supported by the summed(or averaged) values for a period because time sequence of data is buried in the summation. With an appropriate use of parameters, the proposed method can be utilized in detecting the space and time at risk, with respect to the geographic phenomena such as crime, disease, pollution, and accident.

Reference

Aerts, K., Lathuy, C., Steenberghen, T., and Thomas, I., 2006, “Spatial Clustering of Traffic Accidents Using Distances along the Network,” *Proceedings of the 19th International Cooperation on Theories and Concepts in Traffic Safety(ICTCT) Workshop*. Minsk, Belarus, Oct. 26-27, 2006.

Anselin, L., 1995, “Local Indicators of Spatial Association – LISA," *Geographical Analysis*, Vol. 27, No. 2, 93~115.

Anselin, L., 1996, “The Moran Scatterplot as an ESDA Tool to Assess Local Instability in Spatial Association," in Fisher, M., Scholten, H. J., and Unwin, D.(eds.), *Spatial Analytical Perspectives on GIS*, London: Taylor & Francis, 111~125.

Bailey, T. C. and Gatrell, A. C., 1995, *Interactive Spatial Data Analysis*, Essex: Longman Scientific & Technical.

Bera, R. and Claramunt, C., 2003, “Topology-based Proximities in Spatial Systems," *Journal of Geographical Systems*, Vol. 5, No. 4, 353~379.

Boots, B., 2003, "Developing Local Measures of Spatial Association for Categorical Data," *Journal of Geographical Systems*, Vol. 5, No. 2, 139~160.

Flahaut, B., Mouchart, M., San Martin, E., and Thomas, I., 2003, “The Local Spatial Autocorrelation and the Kernel Method for Identifying Black Zones - A Comparative Approach," *Accident Analysis and Prevention*, Vol. 35, No. 6, 991~1004.

Fotheringham, A. S., 1997, “Trends in Quantitative Methods I: Stressing the Local," *Progress in Human Geography*, Vol. 21, No. 1, 88~96.

Fotheringham, A. S. and Brunsdon, C., 1999, "Local Forms of Spatial Analysis," Geographical Analysis, Vol. 31, No. 4, 340~358.

Geary, R. C., 1954, “The Contiguity Ratio and Statistical Mapping," *Incorporated Statistician*, Vol. 5, No. 3, 115~145.

Getis, A. and Ord, J. K., 1992, “The Analysis of Spatial Association by Use of Distance Statistics," *Geographical Analysis*, Vol. 24, No. 3, 186~206.

Getis A. and Ord J. K., 1996, "Local Spatial Statistics: An Overview," in Longley, P. and Batty, M.(eds.), *Spatial Analysis: Modelling in a GIS Environment*, Cambridge: GeoInformation International, 261~277.

Goodchild, M. F., 1986, “Spatial Autocorrelation," *Concepts and Techniques in Modern Geography(CATMOG)*, No. 47, Norwich: Geobooks.

Hong, S.-K., 1998, “Detecting Space-Time Clusters in Linear Point Data," *Journal of the Korean Geographical Society*, Vol. 33, No. 2, 325~338.

Lee, J. and Wong, D., 2001, *Statistical Analysis with ArcView GIS*, New York: John Wiley & Sons.

Levine, N., Kim, K. E., and Nitz, L. H., 1995, “Spatial Analysis of Honolulu Motor Vehicle Crashes: I. Spatial Patterns," *Accident Analysis and Prevention*, Vol. 27, No. 5, 663~674.

Maher, M. J. and Mountain, L. J., 1988, “The Identification of Accident Blackspots: A Comparison of Current Methods," *Accident Analysis and Prevention*, Vol. 20, No. 2, 143~151.

McGuigan, D. R. D., 1981, “The Use of Relationships between Road Accidents and Traffic Flow in Black-Spot Identification," *Traffic Engineering and Control*, Vol. 22, No. 8-9, 448~453.

Messner, S. F. and Anselin, L., 2004, “Spatial Analyses of Homicide with Areal Data," in Goodchild, M. and Janelle, D.(eds.), *Spatially Integrated Social Science*, New York: Oxford University Press, 127~144.

Moran, P., 1948, "The Interpretation of Statistical Maps," *Journal of Royal Statistical Society*, Vol. 10, No. 2, 243~251.

Nicholson, A. J., 1989, “Accident Clustering: Some Simple Measures," *Traffic Engineering and Control*, Vol. 30, No. 5, 241~246.

Okabe, A., Okunuki, K., and Shiode, S., 2006, “The SANET Toolbox: New Methods for Network Spatial Analysis," *Transactions in GIS*, Vol. 10, No. 4, 535~550.

Ord, J. K. and Getis, A., 1995, “Local Spatial Autocorrelation Statistics: Distributional Issues and an Application," *Geographical Analysis*, Vol. 27, No. 4, 286~306.

Park, K.-H., 2004, “A Study on the Effect of Spatial Proximity Weight Matrices on the Spatial Autocorrelation Measures: the Case of Seoul Administrative Units," *Research of Seoul & Other Cities*, Vol. 5, No. 3, 67~83.

Sabel, C. E., Kingham, S., Nicholson, A., and Bartie, P., 2005, “Road Traffic Accident Simulation Modelling - A Kernel Estimation Approach," *Proceedings of the 17th Annual Colloquium of the Spatial Information Research Centre*, The University of Otago. Dunedin, New Zealand, Nov. 24-25, 2005, 37~41.

Steenberghen, T., Dufays, T., Thomas, I., and Flahaut, B., 2004, “Intra-urban Location and Clustering of Road Accidents Using GIS: A Belgian Example," *International Journal of Geographical Information Science*, Vol. 18, No. 2, 169~181.

Upton, G. J. G., 1990, “Information from Regional Data," in Griffith, D. A.(ed.), *Spatial Statistics, Past Present and Future*, Institute of Mathematical Geography: Monograph 12, Ann Arbor: Michigan Document Series, 315~359.

Wulder, M. and Boots, B., 1998, “Local Spatial Autocorrelation Characteristics of Remotely Sensed Imagery Assessed with the Getis Statistic," *International Journal of Remote Sensing*, Vol. 19, No. 11, 2223~2231.

Yamada, I. and Thill, J.-C., 2004, “Comparison of Planar and Network K-functions in Traffic Accident Analysis," *Journal of Transport Geography*, Vol. 12, No. 2, 149~158.

Yao, X. 2003, “Research Issues in Spatio-temporal Data Mining," *Proceedings of University Consortium for Geographic Information Science(UCGIS) Workshop on Geospatial Visualization and Knowledge Discovery,* Lansdowne, VA, USA, Nov. 18-20, 2003.

원 고 접 수 일 : 2007년 7월 5일
1차심사완료일 : 2007년 7월 24일
최종원고채택일 : 2007년 8월 7일